

Modeling of high-frequency seismic wave propagation via observed waveform and numerical simulations using 3D heterogeneous model

*Shunsuke Takemura¹

1. National Research Institute for Earth Science and Disaster Resilience

To achieve precise modeling of high-frequency (>1 Hz) seismic wave propagation, small-scale heterogeneities, which have characteristic scales less than several kilometers, should be required (e.g., Sato, 1984, 1989; Kumagai et al., 2011; Takemura et al., 2015). In this study, to investigate the effects of small-scale velocity heterogeneity and surface topography on seismic wave propagation, we conducted finite-difference method simulation of seismic wave propagation for shallow moderate earthquake. We conducted FDM simulations of shallow moderate (Mw 4.4) earthquake occurred in the Shimane-Hiroshima boarder on 25 November, 2011. The model covers a volume of $384 \times 384 \times 128 \text{ km}^3$, which is discretized by a uniform grid size of 0.1 km. Technical details are same as in Takemura et al. (2015). The background velocity structure is referred from the Japan Integrated Velocity Structure Model (JIVSM; Koketsu et al., 2012). Small-scale velocity heterogeneity model of Kobayashi et al. (2015) is embedded over the crust of the JIVSM. Intrinsic attenuations of the crust for *P* and *S* waves is represented by a single-relaxation Zener body with $Q_s^{-1} = Q_p^{-1} = 4.0 \times 10^{-3}$ and reference frequency $f_0 = 1 \text{ Hz}$ (Takemura et al., 2017). We assume a double-couple point source referred from the F-net MT catalog. We also conducted FDM simulation using the JIVSM without small-scale velocity heterogeneity (original JIVSM), as a reference. Our simulations well reproduced observed PGV and characteristics of seismic wave propagation for frequencies of 0.1-4 Hz. However, in the original JIVSM, coda waves are excited due to topographic scattering but its envelope shapes doesn't show smooth-time decay. By introducing small-scale velocity heterogeneity, simulated coda envelopes well agree with observed smooth coda envelopes. The effects of small-scale velocity heterogeneity dominate in higher frequencies. Simulated PGVs of JIVSM are widely fluctuated due to the source radiation pattern but this fluctuation is suppressed by homogenizing azimuthal variation of PGVs due to small-scale velocity heterogeneity.

Acknowledgement

We used the Hi-net/F-net data and F-net MT solution. The computations were conducted on the Earth Simulator at the Japan Marine Science and Technology (JAMSTEC).

Keywords: Seismic wave propagation, Small-scale velocity heterogeneity, Irregular topography, High-frequency seismic waves, Numerical modeling

Significant anomalies in high-frequency seismograms for intra-slab earthquakes observed in Kanto area, Japan

*Nozomi Kanaya¹, Takuto Maeda¹, Kazushige Obara¹, Akiko Takeo¹

1. Earthquake Research Institute, The University of Tokyo

In Kanto-Tokai area in Japan, very complicated high frequency seismograms are frequently observed as it is located above a complicated plate boundary zone between the Pacific plate and the Philippine Sea plate. In this study, we found characteristic high-frequency seismogram anomalies potentially being related to characteristic inhomogeneity in this area.

We analyzed 20 intra-slab earthquakes (M4.4–6.9) occurred within the Pacific slab from October 2004 to April 2016, 227–453 km in focal depth. The datasets are velocity seismograms recorded by 258 NIED Hi-net stations in Kanto-Tokai area. After applying bandpass filters of octave bandwidth ranging from 1 to 16 Hz, characteristic wave packets and their frequency dependence are identified from root mean squared (RMS) envelope seismograms. At a frequency range of 8–16 Hz in Kanto area, we found wave packets preceding the arrival of S waves by about 10–20 s. The wave packets lasted about 10 s and their amplitude was obviously larger than that of the P-coda waves. At lower frequency of 1–2 Hz, we did not find similar packets. These wave packets were not observed for intra-slab shallow earthquakes, less than 200 km in focal depth. The amplitude of the packet at high frequency was always predominant in the vertical component. No strong polarization in the horizontal component RMS envelopes is observed.

Complicated-shape wave packets lasting about ten seconds, without significant pulse of boundary conversion, suggest that a sort of scattered wave packets are generated by the small-scale inhomogeneities. In addition, this cannot be explained by a simple S-to-S scattering because the arrival time of the packet precedes that of the direct S wave. Based on the systematic detection, we found that the wave packet propagated almost along the radial direction from the epicenter with almost the same apparent velocity as that of the S waves. Considering the wave packets arrived earlier than S waves, they are expected to involve mode-conversion such as P-to-S or S-to-P scattering, by characteristic inhomogeneity between the epicenter and seismic stations.

We conducted preliminary numerical simulations of seismic wave propagation with a community velocity model in this area superimposed onto a small-scale stochastic velocity fluctuation. The resultant synthetic waveforms did not explain these peculiar wave packets. Considerable updates especially for small-scale inhomogeneities in the velocity model are expected to contribute to further understandings of seismic wave propagation in the subduction zone.

Keywords: seismic wave propagation, scattering, seismogram envelope, subduction zone, numerical simulation

Comparison of the 3D FD simulation and statistical methods for the scalar wavelet propagation through random media

*Kentaro Emoto¹, Haruo Sato¹

1. Graduate School of Science, Tohoku University

Considering seismic wave scattering due to small-scale heterogeneities is important for the analysis of short-period (<1s) seismograms. The scattering causes the broadening of seismogram envelopes and the attenuation of peak amplitudes with travel distance increasing. There are statistical methods to model these phenomena by considering an ensemble of random media and investigating statistical characteristics of the propagation of a wavelet through random media. In order to synthesize the theoretical envelope of a short-period wavelet, the radiative transfer equation with the Born approximation (RTE+Born) and the Markov approximation based on the parabolic approximation have been developed and applied to the observed data to estimate the statistical properties of the earth medium. Comparison of these methods with the finite difference (FD) simulation of the wave propagation is important to check the validity of each method; however, there have been few studies since the computation cost of the FD simulation in 3D is expensive.

In this study, we conduct 3D FD simulations of the scalar wavelet propagation by using the Earth Simulator, which is a vector supercomputer managed by JAMSTEC. The target frequency is 1.5Hz and the grid spacing is 0.08 km. The average propagation velocity is 4 km/s, so there are 33 grids per a wavelength, which ensure to prevent grid dispersion. Precisions of the differentiation are 4th and 2nd order in space and time, respectively. A model medium is a cube of 307 km each side and the number of grids for each axis is 3840. In order to realize such a large random medium, we smoothly merge small-size random media generated by using different random seeds. We use 6 merged random media in total. We set an isotropic source of a Ricker wavelet at the center of the medium and receivers at propagation distances of 25, 50, 75 and 100km. The velocity fluctuation is characterized by an exponential autocorrelation function where the fractional fluctuation is 0.05 and the correlation distances (a) are 1 or 5 km. First, we compare the stacked mean square (MS) envelopes of FD simulations with those obtained by RTE+Born and those by the improved Markov approximation (Sato, 2016). For the correlation distance of 1 km ($ak_c=2.3$, where k_c is the centered wavenumber), RTE+Born envelopes adequately fit with FD envelopes in entire lapse time. On the other hand, Markov envelopes well model FD envelopes around the peak for the case of the correlation distance of 5 km ($ak_c=12$). In this case, late coda of FD envelopes are well reproduced by RTE+Born. Next we investigate the distribution of squared amplitudes of each trace. We find that the distribution changes from the log normal distribution at the onset to the exponential distribution at coda. For the case of the correlation distance of 1 km, squared amplitudes show the exponential distribution soon after the onset. This means that the random scattered waves are dominant. According to the FK analysis of the FD traces, we found that the squared amplitudes obey the exponential distribution even when the energy flux of scattered waves is not isotropic.

Keywords: Scattering, Finite Difference Simulation, Markov Approximation, Born Approximation

Synthesis of Scalar Wavelet Intensity Propagating through Random Media Having Power-Law Spectrum

*Haruo Sato¹, Kentaro Emoto¹

1. Tohoku Univieristy

Observed short-period seismograms of small earthquakes show envelope broadening of an S-wavelet and excitation of long lasting coda waves although the source duration is very short. Those phenomena are interpreted as result of scattering by earth medium heterogeneities. As a mathematical model, we study the propagation of a scalar wavelet through von Karman-type random media. When the center wavenumber of the wavelet is lower than the corner wavenumber, we are able to synthesize wave intensity by using the radiative transfer equation with the Born approximation. When the center wavenumber is in the power-law spectral range higher than the corner wavenumber, we can synthesize intensity time traces by using the Markov approximation method based on the parabolic/paraxial approximation. This method is effective for the intensity synthesis especially near around the peak arrival; however, it fails to synthesize coda excitation due to wide-angle scattering. Here, developing the scheme given by (Sato, 2016), we newly propose the following method for the synthesis of intensity time trace from the onset through the peak until coda: (1) We divide the random medium spectrum into the high-wavenumber (short-scale) and the low-wavenumber (long-scale) spectrum components by using the center wavenumber of the wavelet as a reference. (2) Applying the Born approximation to the short-scale component of random media, we calculate the scattering coefficient. Substituting the scattering coefficient into the radiative transfer equation with a constant velocity, we calculate the intensity by using the Monte Carlo simulation. (3) Applying the Markov approximation to the long-scale component of random media, we analytically calculate the envelope broadening and wandering factors. (4) We convolve these factors with the intensity calculated in step (2) in the time domain, which leads to the Green function in the random media. As a test, we have compared intensity time traces derived from the above method and the FD simulation method for a Ricker source wavelet radiated from a point source in random media. We have confirmed good coincidence between them from the onset through the peak until early coda. The proposed method will be a theoretical basis for the study of random inhomogeneous velocity structure in the earth medium from mean square envelopes of short-period seismic waves of small earthquakes.

Keywords: scattering of seismic waves, Heterogeneous structure of the earth, wave theory

Seismic wave attenuation in carbonate rocks: challenging but promising parameter for petroleum exploration.

*Fateh Bouchaala¹, Mohammed Yussuf Ali¹, Jun Matsushima²

1. The Petroleum Institute, 2. University of Tokyo

Seismic wave attenuation is an important parameter in geophysical studies, thanks to its sensitivity to physical parameters of the subsurface such as, fluid content, lithology and fractures. So, an accurate estimation of this parameter can help to enhance the geophysical interpretation and also to increase signal to noise ratio of seismic data. However, getting an accurate seismic attenuation profiles is challenging due to its high sensitivity to noise and immaturity of the methodology. The challenge is bigger in the case of carbonate rocks media, due to their high heterogeneity and complex lithology.

In this study we estimate seismic wave attenuation from different oilfields having different locations in Abu Dhabi. The subsurface of this region is mainly composed of carbonate rocks. We implemented a robust processing workflow and we developed a new method, this in order to get an accurate and high depth-resolution attenuation profiles from Vertical Seismic Profiling (VSP) and sonic data. The results show a significant contribution of scattering on total attenuation, this can be interpreted by high the heterogeneity and the complex lithology of carbonate rocks. The scattering and intrinsic attenuation show a sensitivity to fractures, fluid and clay content. This is a good indication about the attenuation potential for reservoir characterization and to enhance geophysical interpretation. The cross plots showed a link between sonic attenuation and petrophysical logs, which means that these latter can be predictable from the attenuation.

The results obtained herein can be improved if we overcome the limitation of the conventional approach, which uses well-log velocities and densities to calculate scattering attenuation based on the assumption that the total attenuation is a linear summation of intrinsic and scattering attenuation. It is important to confirm the validity of the assumption of strong scattering in order to adequately estimate the scattering attenuation from velocity or acoustic impedance data. We proposed a new approach to separate between scattering and intrinsic attenuation based on reforming the modified median frequency shift (MMFS) (Suzuki and Matsushima 2013) method with seismic interferometry (SI) (Matsushima et al 2016) under the assumption that intrinsic and scattering attenuation are frequency independent and frequency dependent, respectively. The numerical results demonstrate the superiority of the proposed method as compared to the conventional approach and the importance of optimizing parameters in the application of preprocessing filters to balance the resolution power and noise reduction effect.

Keywords: seismic wave attenuation, carbonate rocks, fluid and fractures, mechanism

Strong Land-Atmosphere Coupling in Low Frequency Band below 0.05 Hz

*Toshiro Tanimoto¹, Anne Valovcin¹, Jiong Wang¹

1. Department of Earth Science, University of California, Santa Barbara, CA93106, USA

There are now many arrays that have co-located seismometers and barometers. They provide new opportunities to examine the nature of coupling between the atmosphere and the solid Earth. We will discuss some basic characteristics of the coupling that we learned from the Earthscope Array when we analyzed hurricane data.

In our recent paper (GRL, 43, Geophys. Res. Lett., 43, 2016, doi:10.1002/2016GL070858), we showed that there is a threshold pressure for the coupling between atmospheric pressure and vertical seismic motions; below this threshold pressure vertical amplitudes are flat and are irrespective of local atmospheric pressure. Above this pressure the local atmosphere pressure directly controls vertical amplitudes. This applies only to a low frequency range, below about 0.05 Hz, but for such a low frequency band, correlation between vertical displacement and pressure becomes very high. The correlation coefficients (with zero time shifts) are about 0.8-0.9. In a higher frequency range than 0.05 Hz, such a high correlation does not occur; for example, for 0.1-0.4 Hz which is a secondary microseismic frequency band, amplitudes (noise) are generated in the ocean and are irrelevant to the local atmospheric pressure.

As an interesting display of this characteristics, we will show an example from a hurricane. When Hurricane Isaac (2012) moved over some stations in the Earthscope Transportable Array, pressure and seismic data showed clear effects of vanishing amplitudes near the center of this hurricane for a frequency band below 0.05 Hz. Both pressure and seismic time series showed vanishing amplitudes, appearing like data gaps, if the hurricane center moved over a station almost exactly (within less than 10km). But for stations away from the hurricane track by more than 50 km, such gap-like features were not seen. This may not be surprising for barometer data as pressure is known to be small near the hurricane center but vertical seismic amplitudes also showed similar small amplitudes. This is of course related to a high correlation between pressure and vertical displacement in a low frequency band. Such gap-like features were not found for higher frequency bands.

This feature is somewhat counter-intuitive for a seismologist as we tend to think that the generated low-frequency seismic waves should propagate from a high atmospheric pressure region. Such waves should reach the center of a hurricane and cause some seismic signals. There may be some such signals but the data show that they are quite small; what we observe are highly correlated vertical seismic motion with the local pressure, an almost perfect phase-to-phase match.

Keywords: Land-Atmosphere coupling, Seismic and barometer array

Source locations of Rayleigh waves in secondary microseisms inferred from polarization analysis of Hi-net data

*Ryota Takagi¹, Kiwamu Nishida²

1. Research Center for Prediction of Earthquakes and Volcanic Eruptions, Graduate School of Science, Tohoku University, 2. Earthquake Research Institute, University of Tokyo

Microseisms are energetic ambient seismic wavefield generated by ocean swells, which are categorized into primary (10-14 s) and secondary microseisms (5-7 s). Although observation and application, such as seismic interferometry, of microseisms have been established well, source locations of secondary microseisms still remain uncertain. In the present study, we locate dominant source locations of Rayleigh wave microseisms observed in the Japan islands using Hi-net records. In order to locate microseism source, we first estimate back azimuths of Rayleigh waves in the period of 4-8 s based on polarization analysis. Since fundamental Rayleigh waves, dominating secondary microseisms, generally show retrograde particle motions, back azimuth of Rayleigh waves can be determined without uncertainty of 180 degrees from three component records at single stations. We then search locations explaining the back azimuth distribution, and select source locations with small location errors. The dominant sources of Rayleigh waves mainly distribute in two specific regions: 100-200 km off the coast of Fukushima in the Pacific and off Tottori in the Sea of Japan. The off Tottori sources show a clear seasonal variation, existing only in the winter season. In contrast, the off Fukushima sources are detected stationary. The seasonality is consistent with ocean wave activity in the sea near Japan predicted by an ocean action model WAVEWATCH III. The observation suggests that Rayleigh waves in secondary microseism are dominated by contribution from adjacent sea. The off Tottori and off Fukushima sources are located at an ocean basin with the depth of 1000-2500 m and at shelf slope with the ocean depth of 2000-6000 m, respectively. The oceanic depths are close to the resonance depth of 1500-3000 m for the period of 4-8 s. Improving source locations and investigating their frequency dependence may deepen our understanding of mechanism of microseisms.

Keywords: Microseisms, Surface waves

Global source locations of P-wave microseisms using Hi-net data from 2005 to 2011

*Kiwamu Nishida¹, Ryota Takagi²

1. Earthquake Research Institute, University of Tokyo, 2. Tohoku University

Observations of microseisms date back to the early 1900s [Wiechert 1904]. Although observations of microseisms were firmly established, the excitation mechanisms are still in debate. According to the typical frequency, they can be categorized as primary microseisms (0.02-0.1 Hz), and secondary microseisms (0.1-1 Hz). The former frequency range corresponds to that of ocean swell itself, whereas the latter corresponds to double the frequency of ocean swell. Excitation of primary microseisms can be attributed to linear forcing by ocean swell through the topography in shallow depth, whereas that of secondary microseisms can be attributed to non-linear forcing by standing ocean swell at the sea surface in both pelagic and coastal regions.

The source distribution of secondary microseisms is crucial for understanding the excitation mechanism of secondary microseisms. A back projection method is feasible for locating secondary microseisms. However, complex wave propagations of surface waves caused by strong shallow, lateral heterogeneities prevent from the precise location of the sources. In contrast, body wave microseisms are less scattered than the surface-wave microseisms. Although the amplitudes of body wave microseisms are smaller than surface wave amplitudes, recent developments in source location based on body-wave microseisms enable us to estimate precise locations of forcing and the amplitudes quantitatively [e.g. Nishida and Takagi, 2016].

In this study, we made a catalogue of P-wave microseisms by array analysis using the high-sensitive seismograph network (Hi-net) operated by NIED from 2005 to 2011. We analyzed vertical-component velocity-meters with a natural frequency of 1 Hz at 202 stations in Chugoku district. The instrumental response was deconvolved by using an inverse filtering technique [Maeda et al. 2011] after reduction of common logger noise [Takagi et al. 2015]. The records were divided into segments of 1024 s. After exclusion of segments which include transients, the frequency-slowness spectra were calculated. The spectra at 0.15 Hz show that clear teleseismic P-wave microseisms on seismically quiet days when local swell activities were calm. The local maxima of the spectra were picked up. The centroids of the sources were located by backprojecting the corresponding slowness. The source locations show clear seasonal variations. In winter months, they were located in the northwestern Pacific, and in the summer months, they were located in the southern Indian ocean. Through the years, centroids stayed in the north Atlantic ocean, although they show a weaker seasonal variation with the maximum in winter. The locations can be explained by an ocean action model (WAVEWATCHIII: Ardhuin et al. 2011). In further studies, we will calculate the equivalent vertical single force for quantitative discussions.

Keywords: microseisms, ocean swell, P wave

Multi-mode phase speed measurements of surface waves with array-based analysis

*Hitoshi Matsuzawa¹, Kazunori Yoshizawa^{1,2}

1. Graduate School of Science, Hokkaido University, 2. Faculty of Science, Hokkaido University

Recent deployment of dense broadband seismic networks, such as USArray in the United States, leads to the construction of improved 3-D upper mantle models with unprecedented horizontal resolution using surface waves, although many of such dispersion measurements have been primarily based on the analysis of fundamental mode. Higher-mode information can be of great help in the further improvement of the vertical resolution of 3-D models, but their phase speed analysis is intrinsically difficult, since wave trains of several modes are overlapped each other in an observed seismogram. In case of Love waves, even the fundamental mode tends to be overlapped with higher modes, which result in larger uncertainties in the phase speed measurements of the fundamental-mode Love waves than those of Rayleigh waves. Modal separation is not a straightforward issue because several higher-modes share similar group speeds, but it can be done by utilizing a dense seismic array. In this study, we develop an efficient method for measuring the phase speeds of the fundamental- and higher-mode surface waves based on an array-based analysis, and demonstrate its utility through extensive synthetic experiments and its application to USArray.

Our array-based analysis of multi-mode dispersion measurements is modeled on a one-dimensional frequency-wavenumber method originally developed by Nolet (1975, GRL), which can be applied to broadband seismic records observed in a linear array along a great circle path. At first, proper seismic signals are extracted using varying group-speed windows and slant-stacked with a fixed wavenumber to generate a “beam”. Since the spectrum of this beam is a function of frequency f , phase speed c and group speed U , we can construct spectrograms in c - U domain for each f . After the reduction/removal of spurious spectral peaks by applying narrow wavenumber filter to the largest spectral peaks, the spectrograms in c - U domain are projected in a c - f domain, which eventually provides us with multi-mode dispersion curves.

Extensive sets of synthetic experiments suggest that the method works well for a long linear array with lateral extension of several thousand kilometers. Estimated dispersion curves in the period range between 20 and 150 seconds using a heterogeneous array (i.e., an irregularly distributed stations) reflect an average velocity structure beneath the centroid of the array. The dispersion curves are matched well with theoretical estimation from the average structure depending on the station configuration, especially in a period range with sufficiently strong excitation of each mode. In practical applications, the reliability and errors of measured phase speeds can be assessed by using the width of spectral peaks in a c - f plane. This array-based method of multi-mode phase speed measurement can be of help in the reconstruction of 3-D upper mantle structures with enhanced vertical resolution.

Keywords: surface waves, higher mode, seismic array, North America, USArray

How wide is observation range of the developed stress meter ? - Comparison with STS seismometer -

*Hiroshi Ishii¹, Munemitsu Furumoto¹, Yasuhiro Asai¹

1. Tono Research Institute of Earthquake Science, Association for the Development of Earthquake Prediction

The Tohoku earthquake ($M9.0$) occurred on 11 March 2011. STS seismometers in Japan almost scaled out and could not record larger amplitudes of wave forms. However, stress meters and strain meters developed by Tono Research Institute of Earthquake Science (TRIES) could beautifully record wave forms caused by the earthquake. It is important to record long period seismograms for especially earthquakes occurred in sea because we have to estimate if the earthquake causes large Tsunami or not. Therefore, we compared observation ranges among STS seismometer, stress meter and strain meter. We also investigated how large variations can be observed by stress meter and strain meter. The main results obtained are as follows:

1. Stress meter and strain meter have as 10 times wider observation range than STS observation range.
2. Vertical component of the borehole stress meter of TOS borehole station (depth: 512m) recorded maximum amplitude of about 300kPa for the 2011 Tohoku earthquake. However, the stress meter of high sensitivity can record amplitude of about 5 MPa.
3. The stress meter can observe not only stress but also strain. And observation range of stress meters were about 2×10^{-4} , though maximum amplitudes of observed strain were about 5×10^{-5} .
4. It can be concluded that stress meter developed by us can record whole stress seismogram without scaling out even for gigantic earthquake. Therefore, the stress meter is reliable instrument for estimating Tsunami generation, determining magnitude and research of earthquake mechanism.

Keywords: stress meter, STS seismometer, observation range, Tohoku earthquake ($M9.0$), record of maximum amplitude

A smoothing scheme for numerical solutions of the seismic wave equation

*Ryuta Imai¹, Kei Takamuku¹, Hiroyuki Fujiwara²

1. Mizuho Information & Research Institute, Inc., 2. National Research Institute for Earth Science and Disaster Resilience

In seismic wave propagation simulations for the long-period ground motion evaluation, a stable long-term integration is required for the structure model based on the shallow-deep integrated model. However, numerical instability often causes some divergences of calculation in practice. From experience it has been confirmed that some divergences of calculation often occur in the case that the spatial distribution of the structure has locally severe contrast. Therefore, as a method for mitigating numerical instability, it is reasonable to introduce a smoothing scheme in seismic wave propagation simulation. In order not to impair the characteristics of long-period ground motion by the smoothing scheme, it is desirable for the scheme to remove only spatially localized disturbance components of ground motion. In this study we discuss a smoothing scheme for numerical solutions of the seismic wave equation.

The smoothing scheme proposed in this research consists of both of the seismic wave equation and a correction term, which removes short wavelength components of ground motion selectively. The correction term for the smoothing scheme was derived heuristically by formally extending the operation of upwind difference method of advection equation, which is a stabilized method of the advection equation, to the one dimensional wave equation. As a result, we found that the derived correction term is an operator represented by a combination of the Laplacian and the heat equation. In what follows, we refer to the proposed smoothing scheme as a modified equation scheme. The modified equation scheme has the following features:

- (a) It preserves the characteristics of the wave equation (wave propagation speed).
 - (b) It removes short wavelength components of ground motion selectively.
 - (c) It decreases energy moderately after short wavelength components of ground motion are removed.
- In this study, we reveal that the modified equation scheme have the features above by numerical experiments and mathematical consideration of discretization method for the one dimensional wave equation. We also show that it is necessary to properly set a parameter related to the correction term.

Since the correction term added in the modified equation scheme is simple, we can easily apply it to two dimensional or three dimensional wave equation and more general seismic wave equations. By applying the modified equation scheme to two dimensional wave equation and seismic wave equation, it turned out that the modified equation scheme is also available for more realistic problems.

Keywords: seismic wave equation, smoothing scheme, long-period ground motion evaluation

Time-lapse seismic full waveform inversion for monitoring near-surface velocity changes during microbubble injection

*Rie Kamei¹, UGeun Jang², David Lumley¹, Takuji Mouri³, Masashi Nakatsukasa³, Mamoru Takanashi³, Ayato Kato³

1. University of Western Australia, 2. Seoul National University, 3. JOGMEC

Seismic monitoring provides valuable information regarding the time-varying changes in subsurface physical properties caused by natural or man-made processes. However, the resulting changes in the subsurface properties are often small both in terms of magnitude and spatial extent, leading to minimal time-lapse differences in seismic amplitudes and travel time. In order to better extract information from the time-lapse data, exploiting the full seismic waveform information in the data can be critical. We explore methods of seismic full waveform inversion that estimate an optimal model of time-varying elastic parameters at the wavelength scale. The full waveform inversion methods fit the observed time-lapse seismic waveforms with modelled waveforms based on numerical solutions of the wave equation. Using waveform information beyond first arrivals enables full waveform inversion to achieve much higher resolution (wavelength scale) compared to conventional traveltimes tomography (Fresnel zone scale).

We apply acoustic full waveform inversion to time-lapse cross-well monitoring surveys, and estimate the velocity changes that occur during the injection of microbubble water into shallow unconsolidated Quaternary sediments in the Kanto basin of Japan at a depth of 25 m below the surface. Microbubble water is comprised of water infused with air bubbles of a diameter less than 0.1 mm, and may be useful to improve resistance to ground liquefaction during major earthquakes. Monitoring the space-time distribution of microbubble injection is therefore important to understand the full potential of the technique.

The time-lapse data set consists of 17 monitoring surveys conducted over 74 hours which exhibit excellent repeatability, allowing us to analyze small time-lapse changes in the subsurface. We observe transient behaviors in the seismic waveforms during microbubble injection manifested as traveltimes shifts and changes in amplitude and frequency content. Time-lapse full waveform inversion detects changes in P-wave velocity of less than 1 percent during microbubble injection, initially as velocity increases, and then subsequently as velocity decreases. The velocity changes are mainly imaged within a thin (1 m) layer between the injection well and the receiver well, inferring that microbubble water flow is constrained by the fluvial sediment depositional environment. The resulting velocity models fit the observed waveforms very well, supporting the validity of the estimated velocity changes. In order to further improve the estimation of velocity changes, we investigate the limitations of acoustic waveform inversion, and by applying and comparing elastic waveform inversion to the time-lapse data set.

Keywords: Full waveform inversion, Seismic monitoring, Fluid injection

Nonlinear Attenuation Caused by the Wave Interaction in the Near Surface

*Nori Nakata¹, Norman H Sleep²

1. University of Oklahoma, 2. Stanford University

Strong seismic waves produced dynamic stresses that bring the shallow subsurface into nonlinear frictional failure. Therefore, when the dynamic stress of one type of waves is strong enough to reach the frictional failure, the structure cannot hold other types of waves, and hence these waves have to be attenuated. Physically, the anelastic strain rate increases with increasing dynamics stress, and the dynamic stress is proportional to the difference between total strain and anelastic strain. To the first order with frictional rheology, the effective friction bounds the resolved horizontal acceleration. This hypothesis can be tested at single-station seismograms. We select five earthquakes as examples for examining the effect of the nonlinear attenuation: 1992 Mw 7.3 Landers earthquake, 2008 Mw 6.9 Iwate-Miyagi earthquake, 2011 Mw 9.0 Tohoku earthquake, 2015 Mw 8.3 Coquimbo Chilean earthquake, and 2016 Mw 7.0 Kumamoto earthquake. The strong Rayleigh waves generated by the Tohoku earthquake brought rock beneath MYGH05 station into frictional failure, and the high-frequency S waves simultaneously arrived at the station suppressed. We discover the similar wave phenomena occurred at the Coquimbo Chilean earthquake. In the example of the Iwate-Miyagi earthquake, we find that the P and S waves are nonlinearly attenuated. For this example, the boundary of the observed horizontal and vertical acceleration is close to the gravity acceleration since cohesion of near-surface rock is relatively small. During the Kumamoto earthquake sequence, two strong waves hit at a station within 30 hours and modified the condition of the friction.

Interferometric imaging from borehole seismic data with long-term observatory system and vertical seismometer array

*Kazuya Shiraishi¹, Eiichiro Araki¹, Toshinori Kimura¹

1. Japan Agency for Marine-Earth Science and Technology

We applied interferometric seismic imaging with multiple reflections to borehole seismic survey data with airgun shooting. In the conventional primary reflection imaging such as a vertical seismic profile (VSP), we obtain the reflection image around boreholes in a deeper section than receiver locations, but do not obtain the reflection image in wide range including shallower part than receivers. In addition, boreholes are sparsely distributed. The multiple reflections are generally noise in the primary reflection imaging, but they contain much information in both the deeper part and the shallower part. One effective method to utilize them to obtain subsurface image is seismic interferometry. It is a technique to redatum the multiple reflections to all airgun shooting points them as pseudo-primary reflections by means of cross-correlation for each borehole seismic survey data. Then continuous subsurface image can be obtained along airgun shooting lines.

In this study, we use the borehole seismic data in Nankai Trough. One dataset is a walkaway VSP data acquired in 2009 at IODP C0009 site. The vertical seismometer array was temporally deployed by D/V Chikyu using a downhole wireline tool at 16 levels in the borehole, and a tuned airgun array of R/V Kairei was fired along 54 km shooting line. Other datasets were acquired in airgun surveys with the long-term borehole observatory systems installed at IODP C0002 site and at C0010 site. The airgun surveys were repeatedly conducted with tuned airgun array on R/V Kairei in 2013, 2015, and 2016. In this study, we used the dataset in 2016 along a 128-km-long shooting line, NS1. This line is almost crossing three holes: C0009, C0002, and C0010, and it is very close to the shooting line of the walkaway VSP survey at C0009. The distances from C0009 to C0002 and from C0002 to C0010 are about 20 km and 11 km, respectively. In this study, final reflection image was obtained after merging the post-stack migration sections from each borehole dataset. We achieved to obtain the continuous reflection image along the survey line in the shallow part, including the structures in Kumano forearc basin and faults in frontal thrust zone. Integration of the multiple reflection imaging with the primary reflection imaging will be useful to obtain the whole subsurface image from the shallow to the deep. The spatial resolution and artifacts due to the data sparseness should be investigated for further practical applications. Our result shows an important possibility of the reflection imaging from the sparse borehole seismic data for future monitoring surveys, for example, we might be able to image the location of timelapse change on the subsurface section with the long-term observatory system.

Keywords: borehole seismic survey, long-term borehole observatory system, vertical seismometer array, seismic interferometry

Application of full waveform inversion and pre-stack imaging to 2D land seismic data in a complex terrain

*Takao Nibe¹, Shogo Masaya², Susumu Abe³, Shinji Matsuura², Hiroshi Sato⁴, Tatsuya Ishiyama⁴

1. JGI, Inc., 2. INPEX, 3. JAPEX, 4. ERI

Imaging deep structures using land data acquired in complex terrains of Japan often faces problems such as irregularity of topography and variable shallow structures, variation of reflection points caused by crooked-line geometry, irregular shot interval and low signal to noise ratio. Recently, acquisition of long-offset high density data using combination of cable and cable-free systems in complex terrain is standardized in domestic land acquisition. First Arrival Travel-Time Tomography is applied to such data to estimate subsurface velocity structure where conventional velocity analysis is difficult because of the above mentioned problems.

Although Tomography is able to estimate velocity structure accurately, limited resolution is one of the problems in this method. Full Waveform Inversion (FWI) is a method to estimate high resolution velocity structures compared to tomography since the method uses more information in the inversion process where tomography uses only first arrival time. Recently, a lot of applications are reported widely.

We tried FWI on 2D land data acquired in Japan. First, a synthetic study was done using a similar situation of domestic land data including different source wavelets, irregular sampling, etc. Next, the real data case study is done. We finally applied Pre-stack Depth Migration using FWI result as input and verified their capability of imaging deep structures in the complex terrain.

Keywords: Full Waveform Inversion, Velocity estimation, Reflection seismic exploration

Simulation and field studies of the seismic time lapse by ACROSS methodology

*Junzo Kasahara¹, Yoko Hasada²

1. University of Shizuoka, Faculty of Earth Sciences, 2. Daiwa Exploration and Consulting Co.

Introduction

The temporal change of seismogenic zone and the volcanic evolution are the typical examples of time progression problems in earth sciences. The seismic time-lapse technology is used to estimate the change of subsurface in such cases. ACROSS (Accurately Controlled and Routinely Operated Signal System) methodology has been developed by Kumazawa and others since 1994. According to this methodology, the ACROSS seismic sources were built and have been tested by the groups of JAEA, Nagoya University and JMA. We tested the application of ACROSS technology by simulations and the field tests in Japan and Saudi Arabia.

The authors have applied this methodology for the monitoring of CCS (Carbon Capture and Storage), and EOR (Enhance Oil Recovery). We tried to image the changing zone by the backpropagation of residual waveforms before and after some temporal change in subsurface (Kasahara and Hasada, 2016). In this presentation, we introduce the recent advances of the ACROSS application.

ACROSS methodology

The typical signal used by the ACROSS seismic source is chirp signal within the desired frequency range. By the deconvolution of observed waveforms by the source signature in frequency domain, the transfer function can be calculated. Enhancement of S/N can be obtained by stacking of data during long duration owing to the steady control and the strict synchronization of the source and recording devices.

Detection and imaging of temporal changes

We carried out the field experiment in Awaji Island in 2011 using an ACROSS seismic source with air injection to the 100 m depth during 5 days (Kasahara et al., 2012). Because of excellent repeatability of source signature of the source, the residual waveforms before and after the injection show almost no temporal change before injection and large waveform changes after the injection. We attempted the imaging of the temporal change by backpropagation or reverse-time migration using the residual waveforms.

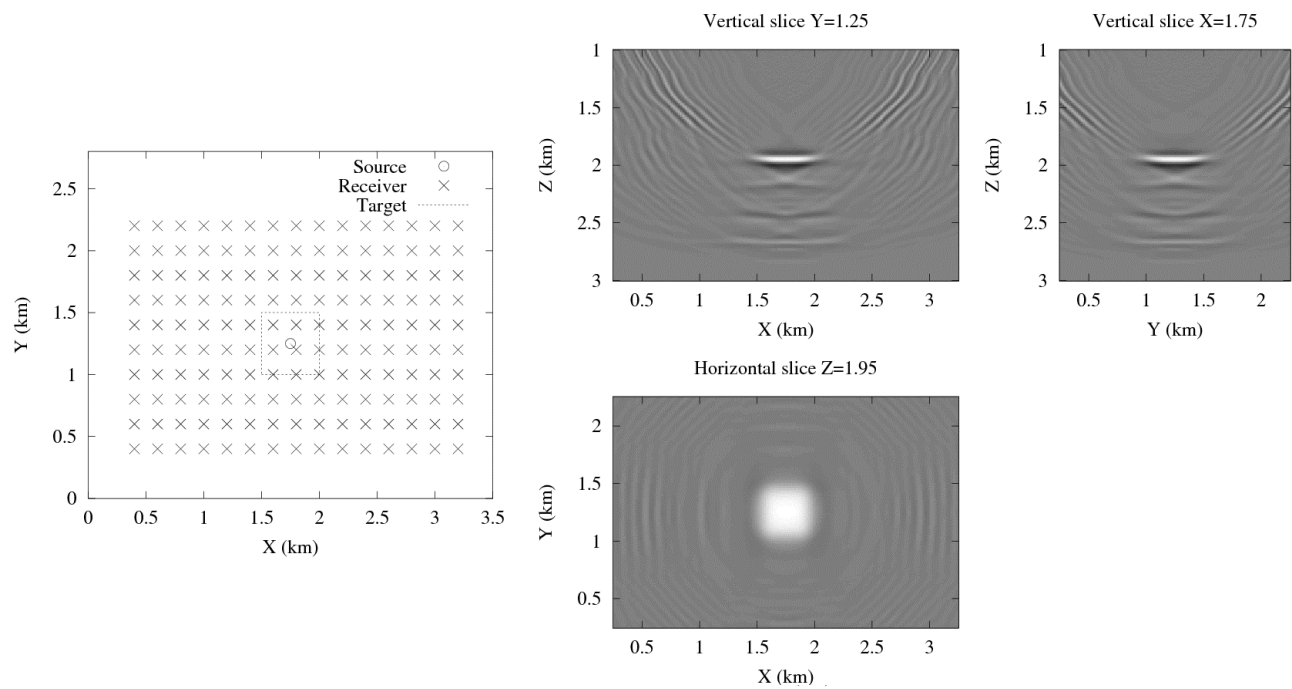
Another field experiment using the ACROSS seismic source was held in Saudi Arabia. We detected temporal changes possibly due to water movement in the aquifers. We discussed the repeatability of observed system and concluded that the repeatability using ACROSS seismic source was the excellent (Kasahara et al., 2016),

We also carried out several simulations in some cases to investigate the effective source and receiver arrangement for subsurface imaging (see figure).

Conclusions

We examined the time-lapse study using the ACROSS seismic source by field tests and simulations assuming a few sources and a dense seismic array (Kasahara and Hasada, 2016). Through field studies and simulations, we showed the temporal changing zone by the backpropagation of residual waveforms. Although we studied the time lapse in a few km scales, this technology can be applied to many cases such as seismogenic zones, volcanic region, civil engineering such as road, river levees, bridges, tunnels and buildings.

Keywords: time lapse, ACROSS, residual waveform, backpropagation, imaging, temporal change



The model setting (left) and the result (right) of the simulation assuming a 2 km deep reservoir.

Detection of spatio-temporal changes of seismic scattering properties with seismic interferometry: Dike intrusion event on 15 August 2015 at Sakurajima volcano

*Takashi Hirose¹, Hisashi Nakahara¹, Takeshi Nishimura¹

1. Department of Geophysics, Graduate School of Science, Tohoku University

In recent years, seismic interferometry has been used to detect spatio-temporal changes of seismic scattering properties (e.g. Obermann et al. 2013a). At Sakurajima, a dike intrusion took place on 15 August 2015, and large ground deformation was observed (e.g. Hotta et al. 2016). Such a dike may work as a new scatter for seismic waves. Therefore, we applied seismic interferometry to detect spatio-temporal changes of seismic scattering properties associated with this dike intrusion. We used the vertical components of ambient seismic noise data at 1 –2 Hz recorded at 6 JMA stations from 1 January 2012 to 31 August 2015. We calculated coherences between reference CCFs (stacked over 2012 and 2013) and daily CCFs, and found that all station pairs showed significant decreases of coherences before and after the dike intrusion. To locate the region where the seismic scattering properties changed, we used sensitivity kernels calculated from 2D radiative transfer model. Parameters of scattering and intrinsic absorption that are needed to calculate sensitivity kernels were estimated by modeling the space-time distribution of energy density of active shot records in 2013. The best-fit parameters were as follows: Mean free path of Rayleigh waves was 1.2 km at 1 –2 Hz, and the value of intrinsic absorption Q was $62.8f$ (f is the frequency). Then, we calculated the differences between mean values of coherence in 2014 (before the event) and those of from 16 August 2015 to 31 August 2015 (after the event) (hereafter called ΔC). Assuming that one seismic scatterer appeared on the surface projection of the dike, we searched the best location of the scatter to explain observed ΔC . As a result, such region was located at the same place as the dike determined by using GNSS, tilt, and strain data (Hotta et al. 2016) with an accuracy of about a few km, and the amount of change of scattering coefficient (Δg) was estimated to 1.4 km^{-1} . These results indicate that seismic interferometry is one of useful methods to detect structural changes of volcano.

Acknowledgements: We used seismograms recorded by JMA. Active seismic experiments were conducted by DPRI, Kyoto University, other 8 universities, and JMA.

Keywords: seismic interferometry, seismic scattering property change, Sakurajima volcano

Analysis of the vibration structure of a hypocenter using a singular value decomposition method

*Toshiaki Kikuchi¹

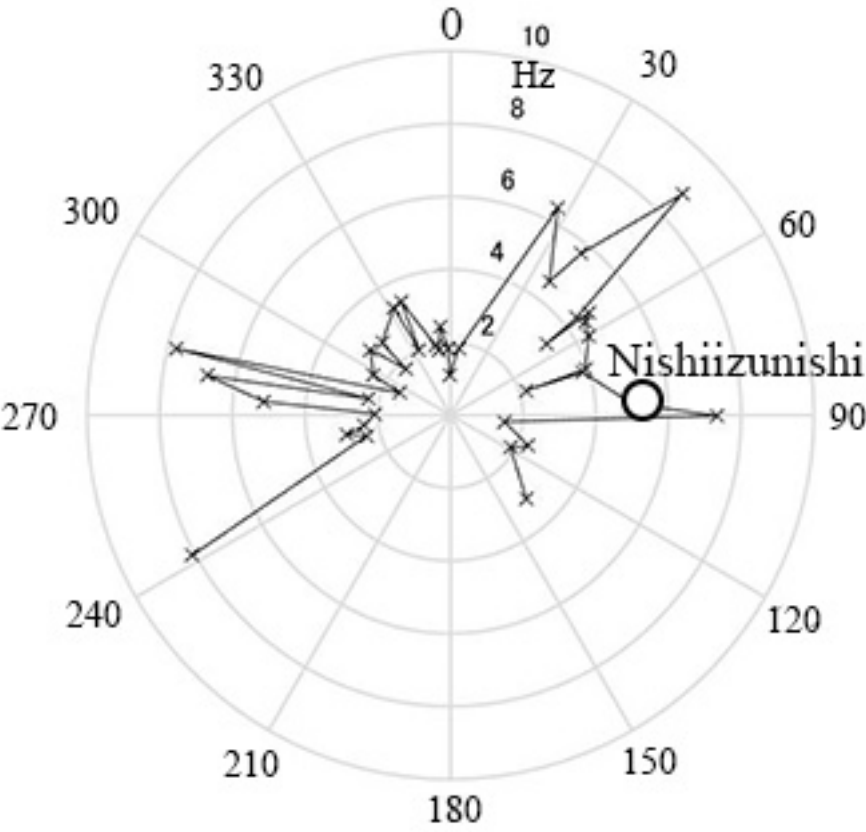
1. National Defense Academy

The vibration structure of a hypocenter are analyzed using a singular spectrum analysis. Specific radiation characteristics related to a hypocenter structure from the results become apparent. The specific radiation characteristics are confirmed for five earthquakes including Kumamoto earthquake. The analysis process is carried out in two stages of the acquisition of equivalent hypocenter vibrations using a time reversal method and the singular spectrum analysis of acquired hypocenter vibration. First, a P wave is cut out from a seismic wave received at an observation station surrounding a hypocenter, and the signal obtained by inverting the time axis of the signal is radiated on a propagation simulation to obtain a pulse formed at the hypocenter position.

At this time, a propagation environment is changed to obtain the condition that the amplitude of a pulse becomes maximum, and the condition is set as the optimum propagation environment. Next, a time reversal pulse (TRP) that is, equivalent hypocenter vibration obtained on the best propagation environment, is analyzed. Since the TRP is a complex oscillating nonlinear signal consisting of multiple frequencies, it is analyzed using a singular value decomposition method. The matrix of time interval dt that consists of n points that consists of the TRP corresponding to an observation station is created. Next, the second matrix that delayed the entire matrix by dt is created. In addition, the third matrix that delayed second matrix by dt is created. This process is repeated m times to obtain a matrix of $m \times n$. The final matrix is an orbital matrix \mathbf{X} . Singular value W is obtained solving the following expression, $\mathbf{X} = \mathbf{U}\mathbf{W}\mathbf{V}^T$. Here, \mathbf{U} and \mathbf{V} are orthonormal matrices satisfying the equation, $\mathbf{U}^T\mathbf{U} = \mathbf{V}^T\mathbf{V} = \mathbf{E}$ (\mathbf{E} : unit matrix). The largest singular value in the W is assumed to be a main component. Here, the earthquake of M6.5 that occurred in the southern part of Suruga Bay on August 11, 2009 was analyzed. First, a P wave is cut out from a signal received at the observation station located around Suruga Bay, and the time axis of the signal is reversed. The reversed signal are radiated from the observation station on the propagation simulation and the pulse (TRP) at the hypocenter location is formed. The singular value decomposition method is applied to the TRP to calculate the components constituting the pulse, and the component with the largest amplitude among them is obtained. The determined main component is a gently fluctuating pulse consisting of almost a single frequency. Likewise, the singular value decomposition method is applied to the TRP corresponding to each observation station, and the component with the largest amplitude is extracted. The frequencies of these components are shown in the figure as a distribution to the azimuth of observation stations centered on the hypocenter. Obviously, the radiation frequency from the hypocenter shows a directivity greatly different depending on the azimuth. That is, the frequency from Susono with the azimuth of 27.4° to Kawadu with the azimuth of 97.0° is high.

These radiation patterns are considered to be related to the vibration mode of active faults.

Keywords: Hypocenter vibration, Time reversal method, Singular value decomposition



The summary of Wave Features Theory of 2011.2.NZ Earthquake Motion.(The same as URAYASU CITY of The TOHOKU Great, The 1964 NIIGATA Earthquake.)

*Masaru Nishizawa¹

1. none

I . PREFACE: had summarized wave features theory of 2011.2.NZ Earth quake Motion. In this area, many seismoments are mstalled. As a result, 9easily summarized wave features theory. City of the 2011 TOHOKU Great Earthquake and The 1964 NIIGATA Earthquake.

II . The Wave Features Theory

- (1) V(vertical)this wave features are closely related to the normal wave features. A and B wave features appears soft ground states.
- (2) The excellent period is about 0.2 sec, therefore $f=1/f$ this fregurency is high considerably. But the period of the A and B is 4 or 5 times.
- (3) The fregurencie of V in completely different from A, B. As thus result, phase shift gres rise to amatter of course. On the CTV building, some supernatural power seems to be at work.
In this short, the complicated oscillation and sotation (twis acr on bwdings, moreover coming ont top of Rayleigh wave actions.
- (4) The horizontal rayleigh wave features shows many reversal of phase. As a result, the building satate on an ventical axis. This setation (twist) is very important force. Of course, CTV building. (Reference. Masaru NISHIIZAWA : The strong spectrum of resemblance between frontier spectrum and Phase difference spectrum of the seismic wave. (Science of form) 2016, JpGU,S-SS25-P35.
This notation force is one of the importance pf the phase spectrum.
- (5) (+)Acceleration and (-)Acceleration indicates different values. Namely, A,B,U acceleration together (+)acceleration indicates higher values than (-) one. This fact indicates the existence of the firm ground than the appear ground. This is the difference of the reflection between firm and soft ground.
- (6) I Think that the thickness of the soft ground in soft is not all by my fair judgment by observing wave features of the soft ground.
- (7) The same distance from the center from the center of the earthquake, though the time of arrival in exists different observation point . This reason is that the spead of the wave of soft ground in slow generally than the firm one.

Abstract:

Because of soft ground, Phase of seismic wave devided from correct behavior and generated rotation (twist) arownd CTV Building (the buildings).

This factor of this rotation (twist) in the phase shift or reversal of phase. This is one of the importance of the phase spectrum.

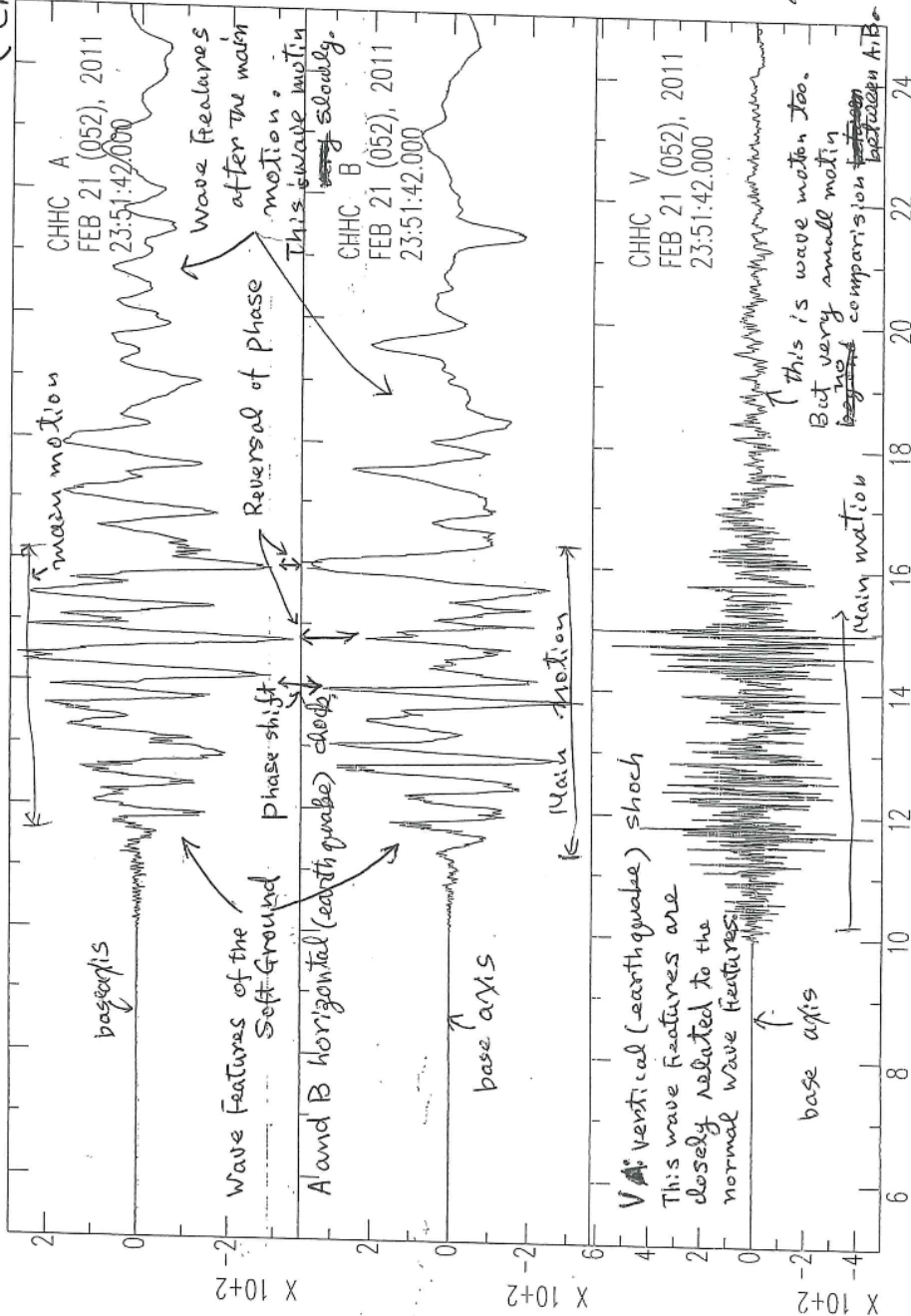
The wave Features of Christchurch.

73 波の形
(Christchurch)
(Wave features)

の東部、南東
波の位相は逆転
している。他と同
いず、水圧(水)に
関係、に2つ(1. 回転
力(2は水圧)が主
いず、2つ(1. 2つ)

の主要電力以後の
波の形は波の2つ
の2つは他と同
事。

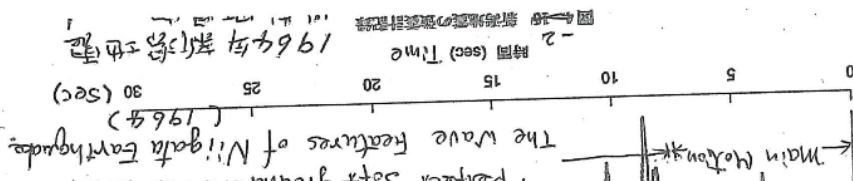
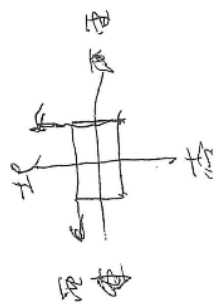
しかし、上下動も
多少は波の2つ(1. 2
つ、2つ、波の2つ
の2つは他と同



(電圧 距離 8 km)

(+) amount of SA, B, V acceleration is high

than (-) amount acceleration. This fact point out existence of a hard type of the ground than this soft ground. And this soft ground is not thick layer of this.



Surface wave characteristics from ambient seismic noise in Northern China

*Yiqiong Li¹

1. Institute of Geophysics, China Earthquake Administration

Studies have shown that the western Taiwan coastal plain is influenced by long-period ground motion from the 1999 Chi-Chi, Taiwan, earthquake, and engineering structures with natural vibration long-period are damaged by strong surface wave in the western coastal plain. The thick sediments in the western coastal plain are the main cause of the propagation of strong long-period ground motion. The thick sediments similar to in the western coastal plain also exist in northern China.

It is necessary to research the effects of thick sediments to long-period ground motion in northern China. We extract surface wave from ambient seismic noise in Northern China and analyze frequency spectrum of surface wave. Our purpose is to reveal the formation and propagation of long-period surface wave in thick sediments and to grasp the amplification effect of long-period ground motion due to the thick sediments.

Keywords: Surface wave, Ambient seismic noise, Thick sediments

Relationship between P wave velocity change and pore water pressure variation induced by the 2016 Kumamoto Earthquake

*Takahiro Kunitomo¹, Hiroshi Ishii¹, Yasuhiro Asai¹

1. Tono Research Institute of Earthquake Science, Association for the Development of Earthquake Prediction

We developed a compact seismic source suitable for high frequency underground survey with the use of the giant magnetostrictive actuator (GMA). This giant magnetostrictive seismic source is composed of a controller system and a vibration exciter driven by a GMA. The controller system generates driving current for a GMA with arbitrary wave form in synchronization with a GPS clock. The vibration exciter generates single force in vertical direction with maximum generating force of 91kgf. This system is currently used to observe mainly P wave velocity change of the bedrock (Toki granite) in 100-200Hz frequency range, because the sampling frequency of the A/D converter in the comprehensive borehole crustal activity observation device is 400Hz. Even at observation points 700m away from the seismic source, it is possible to observe changes in P wave travel time with accuracy of about $10\mu\text{s}$ by stacking for 1 day.

Stepwise travel time delay of the direct P wave, induced by the Kumamoto earthquake (April 16, 2016, Mj7.3), is observed at TGR 350 (distance 353m, about $25\mu\text{s}$ delay) and TRIES (distance 690m, about $60\mu\text{s}$ delay) shortly after the start of continuous transmission. These travel time delays are thought to be caused by the decrease in P wave velocity due to opening cracks in Toki granite. Coseismic and postseismic travel time change of the direct P wave detected at TRIES is consistent with the long-term fluctuation pattern of pore water pressure observed at STG200N in the shaft of the Mizunami Underground Research Laboratory (JAEA). The pore water pressure in the granite rose gradually after stepwise rising at the time of the earthquake, peaked at the beginning of June (about 30kPa), and then gradually dropped. Direct P wave travel time is delayed gradually after the stepwise delay on the day of the earthquake, delayed to about $90\mu\text{s}$ at the same time as the pore water pressure peak, and then gradually recovered. If the pore water pressure rise of 10kPa is converted into the travel time delay of $30\mu\text{s}$, they coincide with each other within the margin of the travel time change estimated error over several months. This result indicates that the pore water pressure changes in the Toki granite controls the opening and closing of the crack and the P wave velocity changes.

Keywords: giant magnetostrictive seismic source, P wave velocity change, pore water pressure, crack, granite

Detection of the changes in elastic wave characteristics in the model slope before and during shallow landslides

*Issei Doi¹, Hironori Kawakata², Masayuki Nakayama², Naoki Takahashi³, Takahiro Kishida⁴

1. Disaster Prevention Research Institute, 2. College of Science and Engineering, Ritsumeikan University, 3. SUMITOMO MITSUI CONSTRUCTION CO., LTD, 4. SMC Tech.

In order to reduce the damages due to shallow landslides, it is effective to construct an early warning system. We pay attention to the use of elastic waves which was used for the rock behavior before the main rupture (Yoshimitsu et al., 2009; Yoshimitsu and Kawakata, 2011). As a first step, we conducted a model test for propagation characteristics of elastic waves before and during shallow landslides.

Landslides occurred 4, 23, and 26 minutes after the initiation of the experiments. The travel times of the elastic waves got larger at the starting time of precipitation and ten minutes before one landslide. These facts suggest that it is possible to monitor the moisture situation and the small deformation of the slope using elastic waves.

Application of seismic interferometry to attenuation estimation on zero-offset vertical seismic profiling data

*Jun Matsushima¹, Mohammed Y. Ali², Fateh Bouchaala²

1. School of Engineering, The University of Tokyo, 2. The Petroleum Institute, Abu Dhabi

Although seismic attenuation measurements have great potential to enhance our knowledge of physical conditions and rock properties, their application is limited because robust methods for improving both the resolution and accuracy of attenuation estimates have not yet been established. In general, it is difficult to improve both the resolution and accuracy of attenuation estimates because there is a relationship of trade-off between them. Thus, the development of a robust method for improving both the resolution and accuracy of attenuation estimates is important. A zero-offset VSP measurement is considered to be best suited for attenuation studies as it enables sampling of the downgoing wavefield at various known depths because the downgoing waveform in a zero-offset VSP data set provides direct observations of the changing nature of the source wavelet as it propagates through the Earth. We propose attenuation estimation methods for zero-offset vertical seismic profile (VSP) data by combining seismic interferometry (SI) and the modified median frequency shift (MMFS) method developed for attenuation estimation using sonic waveform data. One important advantage of the application of SI to seismic exploration is that it allows flexibility of the source and receiver configurations. For example, this means that by applying SI to two different seismic traces recorded at different receivers, a new seismic trace with one receiver acting as a source (virtual source) and the other acting as a receiver can be created. The configuration of zero-offset VSP data is redatumed to that of the sonic logging measurement by adopting two types of SI: deconvolution interferometry (DCI) and crosscorrelation interferometry (CCI). Then, we can apply the MMFS method to the redatumed VSP data. Although the amplitude information estimated from CCI is biased, we propose a correction method for this bias to correctly estimate attenuation. First, to investigate the performance both in resolution and accuracy, we apply different trace separations to synthetic data with random noise at different signal-to-noise ratio (SNR) levels. Second, we estimate the influence of residual reflection events after wavefield separation on attenuation estimation. The proposed methods provide more stable attenuation estimates in comparison with the spectral ratio (SR) method because the mean-median procedure suppresses random events and characteristic features caused by residual reflection events in spectral domain. Our numerical experiments also demonstrate that the MMFS methods identify impulsive attenuation values caused by transmission loss due to reflection at an interface while such impulsive values are not observed in SR methods. This is because the SR method derives attenuation estimates based on frequency component change between two receiver depths while the MMFS method uses the amplitude variation, implying that the proposed methods can estimate scattering attenuation values from amplitude information even if frequency components are not changed between the two receiver depths. By preliminarily applying the proposed methods to field VSP data, we find some differences in the depth resolution and stability of attenuation values between the proposed method and the SR method, demonstrating that the proposed methods are more stable than the SR method especially in the shortest receiver separation. The responses of attenuation results obtained by applying different attenuation estimation methods to field data at different receiver separations correlate with those in our numerical experiments. To further verify and extend the applicability of the proposed method, one of future works should focus on validation of obtained attenuation results by comparing a seismic trace or its spectrum before and after attenuation compensation by inverse Q filtering. In our case, a component of attenuation due to scattering effects is also included in the obtained attenuation estimates and thus such scattering effects should be taken into account in attenuation compensation.

This attenuation compensation process might be used to estimate the scattering effects. To this end, a study to further investigate the response of the proposed methods to seismic scattering effects which are frequency dependent could be useful in providing new perspectives on the usage of the proposed method.

Keywords: Seismic interferometry , Seismic attenuation, zero-offset VSP

Approximate vector sensitivity kernels of coda-wave decorrelation: 2D single scattering

*Hisashi Nakahara¹, Kentaro Emoto¹

1. Solid Earth Physics Laboratory, Department of Geophysics, Graduate School of Science, Tohoku University

Coda-wave interferometry has been used to detect medium changes in association with large earthquakes or volcanic eruptions. It is important to determine the region of these medium changes correctly for understanding physical mechanisms to cause them. For that purpose, sensitivity kernels of coda waves play a crucial role. Regarding travel time changes of coda waves, the sensitivity kernels have been approximately extended to vector waves under single scattering regime by Nakahara and Emoto (2016). Regarding decorrelation of coda waves, the sensitivity kernels have been formulated so far for scalar waves only (e.g. Planes et al, 2014; Margerin et al., 2016). Hence, we try to derive analytical expressions for vector waves in two-dimensional cases. The key point in our simple extension to vector waves is the projection of seismic phonon energy into horizontal and vertical components by using the square of the direction cosine of the polarization direction. This idea is the same as one used in Nakahara and Emoto (2016) for travel-time sensitivity kernels. Thanks to this simple idea, we can derive approximate but analytical expressions of the sensitivity kernels by using the two-dimensional single isotropic scattering model for scalar waves, though we can treat either P waves or S waves at a time. Our results show that the sensitivity kernels are different for different components. They have non-zero values only on the single-scattering shells. There exist points where the kernels have zero amplitudes, and these points are different for the two components. These are theoretically shown by this study for the first time. These sensitivity kernels are helpful for us to know how to use different components simultaneously in coda-wave interferometry.

Keywords: Sensitivity kernel, coda waves, vector waves

Estimation of scattering coefficient and intrinsic absorption in the Chugoku district (2)

Daisuke Takahagi¹, *Jun Kawahara¹, Kentaro Emoto², Tatsuhiko Saito³

1. Ibaraki University, 2. Tohoku University, 3. National Research Institute for Earth Science and Disaster Resilience

It is possible to separately estimate the scattering coefficient and intrinsic absorption of the lithosphere by interpreting the observed spatiotemporal distribution of high-frequency seismic wave energy by the Radiative Transfer Theory (RTT). One of such an estimation method is the Multiple Lapse-Time Window (MLTW) method (Fehler et al., 1992; Hoshiba, 1993; Carcole and Sato, 2010), in which the seismic wave energy observed respectively at different positions is integrated using multiple time windows and then its spatial variation is interpreted by the RTT. Recently, Saito et al. (2013, 2014, Seism. Soc. Jp. Fall Meet.) proposed another method to estimate the scattering coefficient and intrinsic absorption. In this method, the seismic wave energy observed respectively at different times is integrated using multiple space windows and then its temporal variation is interpreted by the RTT. Sasaki et al. (2015a, JpGU Meet.; 2015b, SSJ Fall Meet.) improved this method and applied it to the Hi-net records of several shallow earthquakes in the Chugoku district, Japan. He concluded that the scattering coefficient of S waves (1-2 Hz) in this region is on average 0.002-0.0025 km⁻¹. It is roughly half as large as the values previously estimated in this region using the MLTW method.

In this study, we improved the coda normalization process for correcting the source and site effects in the method of Sasaki et al. Though they assumed that the scattering coefficient (g_0) and intrinsic absorption (Q_i^{-1}) are uniform, we introduced a model such that the crust and the uppermost mantle could have g_0 and Q_i^{-1} of different values. We analyzed the Hi-net data of the same events using the improved method. We obtained the g_0 and Q_i^{-1} for frequency bands of 1-2, 2-4, and 4-8 Hz. The g_0 did not show obvious frequency dependence, but the Q_i^{-1} appeared smaller for higher frequencies. The g_0 values we estimated were significantly smaller than those estimated by the previous studies using the MLTW method for all frequency bands. The choice of g_0 and Q_i^{-1} of the uppermost mantle gave little influence on the results. This is because the ray paths from the shallow events (9-13km in depth) that we selected mostly go through the crust only. To evaluate the g_0 and Q_i^{-1} of the uppermost mantle, we would need to analyze data of deeper events.

Acknowledgements: We used the data by the Hi-net and the dataset of the velocity structure model of Matsubara and Obara (2011), both provided by National Research Institute for Earth Science and Disaster Resilience.

Keywords: seismic wave energy, scattering, intrinsic absorption

Temporal change of subsurface structure near Mt. Aso inferred from seismic interferometry using V-net vertical array data

*Yuta Mizutani², Kiwamu Nishida¹, Yosuke Aoki¹

1. Earthquake Research Institute, University of Tokyo, 2. Univ. of Tokyo

Volcanic activity could be often activated by tectonic stress changes by a large earthquake. For example, Mt. Aso erupted in October 2016 after the 2016 Kumamoto Earthquake. To understand the relation between these events, it is important to monitor the temporal change of the structure of seismic velocity related to the event. In this study, we estimated the temporal change of subsurface structure in the Aso region with seismic interferometry (SI).

Monitoring seismic velocity by SI requires the isotropic source distribution, because the temporal or spatial change of the distribution of the sources biases the measured temporal change of subsurface structure. In order to mitigate the bias, a measurement of the temporal velocity change utilizing coda part of the cross-correlation function (CCF) is feasible. Moreover, the delay time of coda waves is larger than that of the direct waves. This means even a subtle change could be detected from coda waves with high accuracy. Here, we focused on how to localize the temporal subsurface velocity change from the difference between direct waves and coda waves.

In this study, we analyzed the data recorded from January 1, 2015, to October 31, 2016, at 4 V-net stations deployed by National Research Institute for Earth Science and Disaster Resilience (NIED) around Mt. Aso. Each station is composed of a broadband seismometer at the surface and a high-frequency seismometer (1 Hz) at the bottom of a borehole (depth ~200 m). First, the records were bandpass-filtered from 2 to 8 Hz. After one-bit normalization of the records and spectral whitening, a CCF between same components of the bottom and surface sensors was calculated every day. Then, we made a reference CCF by stacking CCFs from October 25, 2016 to October 31, 2016. Second, we measured the delay times between the reference and a CCF in time windows of 2.56 s whose center time was increased from -5 s to 5 s every 0.2 s. Plots of the delay time against lag time show a linear trend. When the temporal change is homogeneous, the slope characterizes the bulk velocity change within a spatial scale of about 2 km. In contrast, the intercept, which represents travel time of direct waves, characterizes the localized velocity change between the station pair (~200 m).

After the 2016 Kumamoto Earthquake, the estimated slope of the EW component showed the velocity reduction of approximately 0.2 % at 3 stations except for Takamori station. At Takamori station, the seismic velocity was little changed in the EW component, but in the NS component, about 0.2 % of the velocity drop was detected. On the local velocity change in the borehole with the depth of about 200 m, nearly 5-8 % velocity drop was observed in the EW component at Hakusui and Ichinomiya stations and the NS component at Takamori station. Otherwise, there was an approximately 20 % drop at Nagakusa station. This could attribute the serious damage of subsurface structure by the earthquake.

At Ichinomiya station, the velocity change with a time scale of a few weeks coincided with that of the precipitation data. This change was well agreed with a simple model of the ground water level inferred from the data. The change could be localized near the borehole, because the detected temporal change was associated with that of water head in a volcanic alluvial fan.

In this study, we detected the temporal velocity change on a scale from several hundred meters to some kilometers using vertical array data. In a future study, we will address CCF analysis with ray paths across Mt. Aso for detecting the temporal change associated with the volcanic event.

Keywords: Seismic interferometry, Temporal change of seismic velocity

Temporal change of subsurface velocity structure associated with the 2016 Kumamoto earthquakes

*Tomotake Ueno¹, Tatsuhiko Saito¹, Kaoru Sawazaki¹, Katsuhiko Shiomi¹

1. National Research Institute for Earth Science and Disaster Resilience

We investigated temporal velocity change of subsurface structure before and after the 2016 Kumamoto earthquakes in April 2016 by applying the seismic interferometry method to ambient seismic noise. We calculated auto-correlation functions (ACFs) of continuous waveforms recorded by Hi-net vertical velocity component after bandpass filter of 1 –3 Hz is applied. Velocity change of subsurface structure was calculated by applying the stretching method (Sens-Schönfelder and Wegler, 2006) to the ACFs for lag times of 1 –5 s and 4 –15 s.

The results using the lag time of 1 –5 s showed velocity increase of 6 % at the N.MSIH station located near the fault just after the Kumamoto earthquakes. This velocity increase remained more than 6 months. The stations of N.OGNH and N.KKCH also showed velocity increase although the velocity increases completely recovered (disappeared) 6 months after the earthquakes. On the other hand, significant velocity decreases from 0.5 % to 6.0 % were obtained at N.ASVH, N.NMNH, and N.TYNH. The decrease recovered partially except for the N.ASVH. The result for the lag time of 4 –15 s showed velocity decreases from 0.5 % to 6 % at N.MSMH, N.TYNH, N.ASVH, N.HKSH, N.NMNH, N.KKEH, and N.SNIH near the after shock area and a induced seismicity area of the 2016 Kumamoto earthquakes.

The N.MSIH station which showed the velocity increase is located where negative volume change was expected by a theoretical fault model of the Kumamoto earthquakes. Actually, a large compressional strain was observed between the KiK-net sensors installed on the surface and at the borehole bottom at N.MSIH (Fukuyama and Suzuki, 2016). We, therefore, suppose that the velocity increase found only near the fault was caused by the static compressional-strain. On the other hand, the velocity decrease found at several stations in wider area would be caused by large dynamic strain-change.

Keywords: The 2016 Kumamoto Earthquakes, Temporal velocity change

Temporal Variation in Seismic Velocity Accompanied by 2011 Tohoku-Oki Earthquake and the Slow Slip Event, on Seismic Interferometry of Ambient Noise

*Miyuu Uemura¹, Yoshihiro Ito², Kazuaki Ohta², Ryota Hino³, Masanao Shinohara⁴

1. Kyoto University, 2. Disaster Prevention Research Institute, Kyoto University, 3. Tohoku University, 4. Tokyo University

Seismic interferometry is one of the most effective techniques to detect temporal variations in seismic velocity before or after a large earthquake. Some previous studies have been reported on seismic velocity reductions due to the occurrences of large earthquakes (e.g., Wegler et al., 2009; Yamada et al., 2010) and preceding them (e.g., Lockner et al., 1977; Yoshimitsu et al., 2009). However, only a few studies accompanying slow slip events have been conducted.

Between the end of January and the occurrence of the largest foreshock on March 9 that preceded the 2011 Tohoku-Oki earthquake, slow slip events and low-frequency tremors were detected off Miyagi (Ito et al., 2013, 2015; Katakami et al., 2016). We apply seismic interferometry using ambient noise to data from 17 OBSs that were installed above the focal region before the 2011 Tohoku-Oki earthquake. All OBSs with three components are short-period seismometers with an eigenfrequency of 4.5 Hz that were deployed off Miyagi between November 2010 and April 2011. Before the analysis, we estimated the original deployment orientation with two horizontal components for 13 OBSs, by using particle orbits of some direct P waves from natural earthquakes, to analyze one vertical and two horizontal components. The method is as follows. First, we applied a band-pass filter of 0.25-2.0Hz in the frequency domain, and compared this with a one-bit technique in the time domain to the ambient noise signal. Second, we calculated Auto-Correlation Coefficients using a 5-s time window with lag time from -30 s to 30 s at intervals of 0.1 s, using seven continuous days of waveforms to make a daily ACF. Third, we stacked up all daily ACFs for the entire time period, to make a reference ACF. Finally, we calculated the Correlation Coefficients between the one-day ACF or the 16-day ACF and the reference ACF.

The results are follows. At all OBSs, the 16 days' CC declined after the SSE initiated and then it recovered in the latter half of the SSE duration. In the region of SSE occurrence, the difference between the absolute and incremental reduction in the 16 days' CC is small. However, in the area of the largest foreshock, the difference is significant. The former 16 days' CC values are suddenly decreasing before the SSE, and the latter 16 days' CC values are gradually decreasing starting around November, or around four months before the largest foreshock. The small difference could be related to the occurrence of SSE, while the large difference could be related to critical conditions preceding the largest foreshock.

Keywords: seismic interferometry, ambient noise

Estimation of seismic velocity changes in response to the earth tide: Noise correlation analysis at 13 active volcanoes in Japan

*Tomoya Takano¹, Takeshi Nishimura¹, Hisashi Nakahara¹

1. Graduate School of Science, Tohoku University

Seismic velocity changes due to a large earthquake have received much attention in recent years to understand the mechanical properties of the shallow structure. Strong motion and stress changes due to crustal deformation are considered as mechanisms of seismic velocity changes, however it is necessary to estimate each contribution to understand the mechanism of velocity change quantitatively. Recently, Takano et al. [2014] and Hillers et al. [2015] estimated velocity changes due to the Earth tide by applying seismic interferometry method to ambient noises to investigate the seismic velocity changes only due to stress. However, there are only two studies, hence we estimate seismic velocity changes in response to the Earth tide using ambient noises recorded at 13 active volcanoes in Japan.

Vertical component of ambient noises recorded by Japan Meteorological Agency at 13 active volcanoes in Japan are analyzed: Tokachidake, Meakandake, Mt. Tarumae, Mt. Usu, Hokkaido-komagatake, Mt. Azuma, Mt. Bandai, Nasudake, Mt. Kusatsushirane, Mt. Ontake, Izuoshima, Miyakejima, Unzenfugendake. We analyzed continuous data for 2 years (2013-2014). For every possible pair combination of stations whose distances are within about 5km, we computed cross correlation functions (CCFs) at dilatational and contractional episodes, respectively. Each episode is defined by dividing observation period according to tidal strain amplitudes computed by GOTIC2 [Matsumoto et al., 2001]. CCFs are then stacked for the dilatational episode and the contractional one. By measuring the phase difference between dilatational CCFs and contractional CCFs, seismic velocity changes due to the Earth tide are estimated. Record sections of CCFs indicate that surface wave might be dominant in ambient noise.

Seismic velocity changes due to vertical component of the Earth tide averaged for all station pairs are estimated to be $-0.02 \pm 0.02\%$ at 0.5-1Hz, $-0.01 \pm 0.01\%$ at 1-2Hz, and $-0.06 \pm 0.01\%$ at 2-4Hz, respectively, while seismic velocity changes due to areal component are estimated to be $0.03 \pm 0.02\%$ at 0.5-1Hz, $0.02 \pm 0.01\%$ at 1-2Hz, and $0.06 \pm 0.01\%$ at 2-4Hz, respectively. Negative values of velocity changes indicate seismic velocity is reduced during the dilatational episode in contrast to the contractional episode. Therefore, it appears that seismic velocity is reduced due to vertical dilatation. It is consistent with the result of Hillers *et al.* [2015]. However, Yamamura et al. [2003] and Takano et al. [2014] detected velocity reduction due to areal dilatation. The two studies analyzed P-wave, while this study and Hillers et al. [2015] analyzed Rayleigh waves. This suggests that the observed velocity changes may differ for the orientation of strain and type of seismic waves analyzed.

Keywords: seismic velocity change, seismic interferometry, earth tide

Globally optimized finite difference method to minimize the angle dependent numerical dispersion.

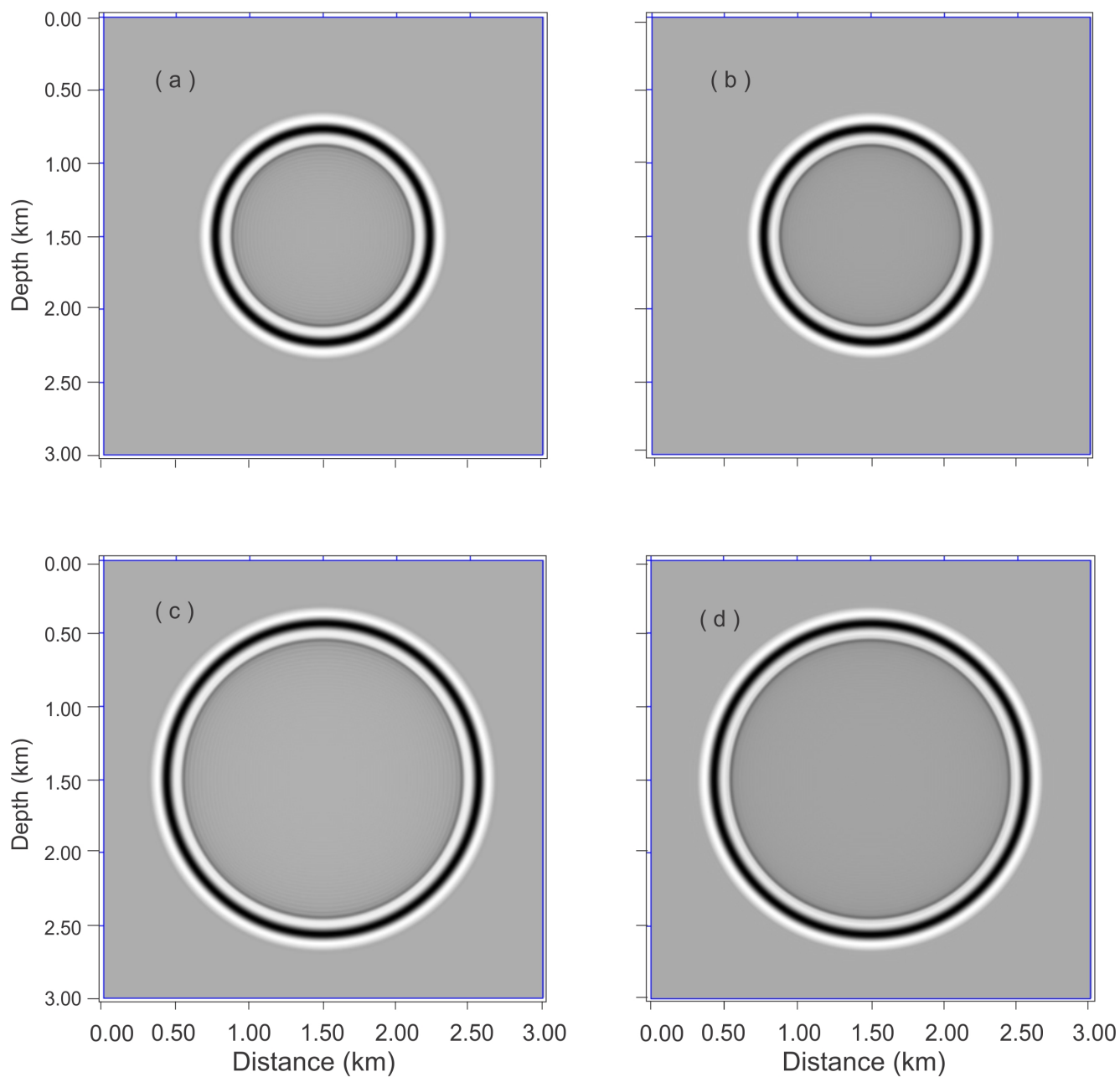
*DEBAJEET BARMAN¹, Dr. MAHESWAR OJHA¹

1. CSIR National Geophysical Research Institute Hyderabad, India

Finite difference modeling is a basic and important tool to solve a differential equation like acoustic wave equation. This method is also used in high resolution seismic imaging. But it faces some challenges for two dimensional wave propagation due to propagation angle dependent numerical dispersion in square grid system. In a conventional Finite Difference Method (FDM), the coefficients are fixed for 1D and 2D propagation. So, with increase of order of approximation the dispersion may be reduced but the non uniformity of dispersion with varying propagation angle retains itself. For existing Pseudo Spectral Method (PSM) using specific window parameter the FD coefficients are constant and is not properly optimized for every angle of propagations.

Here, we propose a method to automatically optimize FD coefficients for every propagation angle. To make the method robust, at first FD coefficients for every propagation angle is optimized by minimizing phase velocity ratio error with reference to the analytic solution using genetic algorithm of certain initial population. Here, the fitness function is generated by the weighted average error in phase velocity ratio for each wave number. As we know that the error in lower wave number should be in higher priority, so we use decay type functions like linear, exponential to calculate the weighted average error by multiplying the function weight with the error at specific wave number. The stability criteria is considered for choosing best of optimized FD coefficients i.e. the FD coefficients whose stability ratio is higher than conventional is considered for the next step for the algorithm. Then final FD coefficients are generated by optimizing from those highly optimized FD coefficients for each propagation angle by genetic algorithm. In the second step, the same stability criteria technique is used for optimization. In second step the FD coefficients are optimized by using fitness function where error is average for every propagation angle. The new method is automated and it does not depend on specific window property like Pseudo Spectral Method (PSM). For some acoustic model PSM technique does not better result for lower order approximation and use of higher order approximation increase the complexity of the method. But in new method there is no such limitation.

Keywords: Genetic algorithm, Phase velocity ratio, Decay function



(a) Conventional 12th order at 500ms, (b) New 12th order at 500ms, (c) Conventional 12th order at 700ms, (d) New 12th order at 700ms velocity 2500m/sec, grid spacing 15m, sampling time 1ms, source is 10Hz Ricker wavelet

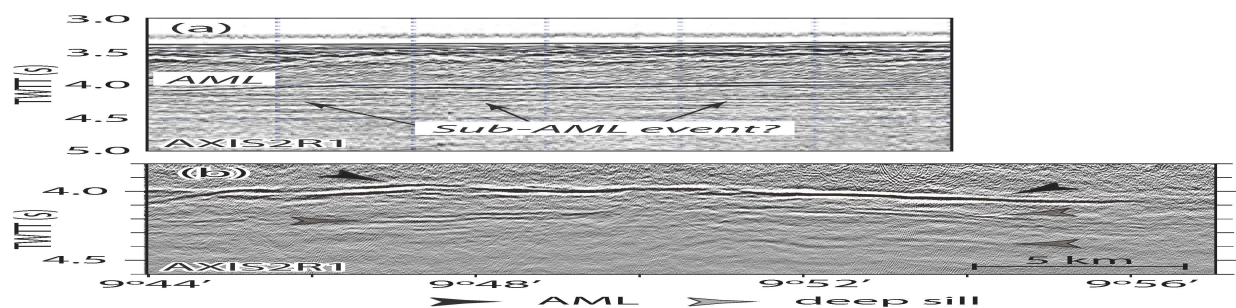
Waveform modeling of the seismic response of a mid-ocean ridge axial melt sill

*Min Xu¹, Wen Yan¹

1. SCSIO, CAS

Seismic reflections from axial magma lens (AML) are commonly observed along many mid-ocean ridges, and are thought to arise from the negative impedance contrast between a solid, high-speed lid and the underlying low-speed, molten or partially molten (mush) sill. The polarity of the AML reflection ($P_{\text{AML}}P$) at vertical incidence and the amplitude versus offset (AVO) behavior of the AML reflections (e.g., $P_{\text{AML}}P$ and S -converted $P_{\text{AML}}S$ waves) are often used as a diagnostic tool for the nature of the low-speed sill. Time-domain finite difference calculations for two-dimensional laterally homogeneous models show some scenarios make the interpretation of melt content from partial-offset stacks of P - and S -waves difficult. Laterally heterogeneous model calculations indicate diffractions from the edges of the finite-width AML reducing the amplitude of the AML reflections. Rough seafloor and/or a rough AML surface can also greatly reduce the amplitude of peg-leg multiples because of scattering and destructive interference. Mid-crustal seismic reflection events are observed in the three-dimensional multi-channel seismic dataset acquired over the RIDGE-2000 Integrated Study Site at East Pacific Rise (EPR, cruise MGL0812). Modeling indicates that the mid-crustal seismic reflection reflections are unlikely to arise from peg-leg multiples of the AML reflections, P -to- S converted phases, or scattering due to rough topography, but could probably arise from deeper multiple magma sills. Our results support the identification of Marjanovic et al. (2014) that a multi-level complex of melt lenses is present beneath the axis of the EPR.

Keywords: East Pacific Rise, Axial melt lens, Waveform modeling, Mid-crustal seismic reflection event, Multiple-sill model



Adjoint tomography beneath the Kanto region using broadband seismograms

*Takayuki Miyoshi¹

1. Earthquake Research Institute, University of Tokyo

The three-dimensional seismic structure in the Kanto region of Japan has been revealed in many past studies, whereas no model with the ability to reproduce observed waveforms is available to aid in the tectonic interpretation of the heterogeneity of the region. We have inferred the three-dimensional seismic wave-speed structure using adjoint tomography (e.g. Miyoshi et al. 2015 SSJ; Miyoshi 2016 JpGU). I report here revised results using the modified procedure from the manner of Miyoshi (2016).

The revisions were following three. (1) I re-determined centroid time. I basically used the parameters of MT solutions provided by the NIED F-net as initial source parameters. Although the synthetics are similar with the observation, the synthetic was faster than the observation on almost seismograms due to significant rupture duration. I estimated the centroid time using the differential time between observation and synthetic estimated by phase correlation for a packet of P-waves. (2) I considered attenuation effect in the forward modeling. I assumed attenuation structure depending on S-wave structure (Olsen et al. 2003). (3) I broaden the period band toward shorter periods. I used four period bands between 5 and 30 sec in the iteration. I started the inversion from the waveforms in the period band of 20 - 30 sec, and finally 5 - 30 sec in order to avoid cycle skipping.

One iteration involved forward modeling, estimation of misfit, calculation of misfit kernel using adjoint method, and model update using Hessian kernels. I obtained the preferred model after 16 iteration. Initial model was the tomographic model based on ray theory (Matsubara and Obara 2011). The main results are as follows: (i) the synthetic waveforms improved 20 % based on the amplitude misfit between observation and synthetics in the period of 5 - 30 sec. The new model reproduced the waveforms of both inversion data and extra data well. (ii) As for average wave-speeds in each depth, the average S-wave speed is not changed basically, while the P-wave speed model was slightly slower than that of the initial model. (iii) I detected the extreme low wave-speed areas at a depth of 5 km and 40 km. These low wave-speed areas are consistent with geological and tectonic features pointed out by the previous researches (e.g. Suzuki 1996; Kamiya and Kobayashi 2000).

Acknowledgements: We thank to the NIED F-net for providing seismological data, and the Computational Infrastructure for Geodynamics (CIG) for providing SPECFEM3D_Cartesian code. This work was supported by JSPS KAKENHI (Grant Number 16K21699) and MEXT KAKENHI (Grant number 15H05832).

Keywords: Seismic wave-speed model, Adjoint tomography, Broadband seismogram

Global features of slabs inferred from regional low- and high-frequency body waves of deep earthquakes

*Yuki Ohata¹, Keiko Kuge¹

1. Department of Geophysics, Graduate School of Science, Kyoto University

We show that high-frequency P and S phases from deep earthquakes arrive at fore-arc stations after low-frequency phases, with increasing delay with thermal parameters in subduction zones. The observation in Tonga may be associated with the metastable olivine wedge (MOW) as well as in northern Japan.

By analyzing features of P and S waves radiated by deep earthquakes, we can elucidate the nature of slabs where the seismic waves have passed. One of the features is difference in arrival time between low-frequency ($f < 0.25$ Hz) and high-frequency ($f > 2$ Hz) signals. This can be observed clearly in the fore-arc side of the volcanic front in northern Japan. Furumura and Kennett (2005) showed that the P and S waves from deep earthquakes beneath the Sea of Japan have low-frequency onsets with high-frequency long-duration signals, suggesting that they are the result of small-scale quasi-laminar heterogeneity within the subducting Pacific slab. The late arrivals of high-frequency P and S signals can be enhanced for earthquakes deeper than 400 km due to the low-velocity MOW in the slab (Furumura et al., 2016).

In this study, we examined seismograms worldwide for the features suggested by Furumura's studies. We collected waveform data of P and S waves from IRIS and F-net broadband seismometers in fore-arc sides of subduction zones where deep earthquakes occur. We measured separation time between low- and high-frequency arrivals. By comparing it with several physical parameters of subduction zones, we found that the separation time could increase with the thermal parameter. The result is consistent with Kennett et al. (2014) who suggested that the quasi-laminar heterogeneity within the oceanic lithosphere can guide high-frequency P_o and S_o waves more efficiently in the older, cold areas of the Pacific. Therefore, the observed correlation between the separation time and thermal parameter may arise from the dependence of the quasi-laminar heterogeneity on temperature. In the areas except for Tonga and northern Japan, we did not find observations that are likely to be evidence for MOW. Large separation time was observed in Tonga, and it tends to be increased for earthquakes deeper than 500 km.

The cause of Mj overestimates ($M_j > M_w$) for the shallow earthquakes in western Japan

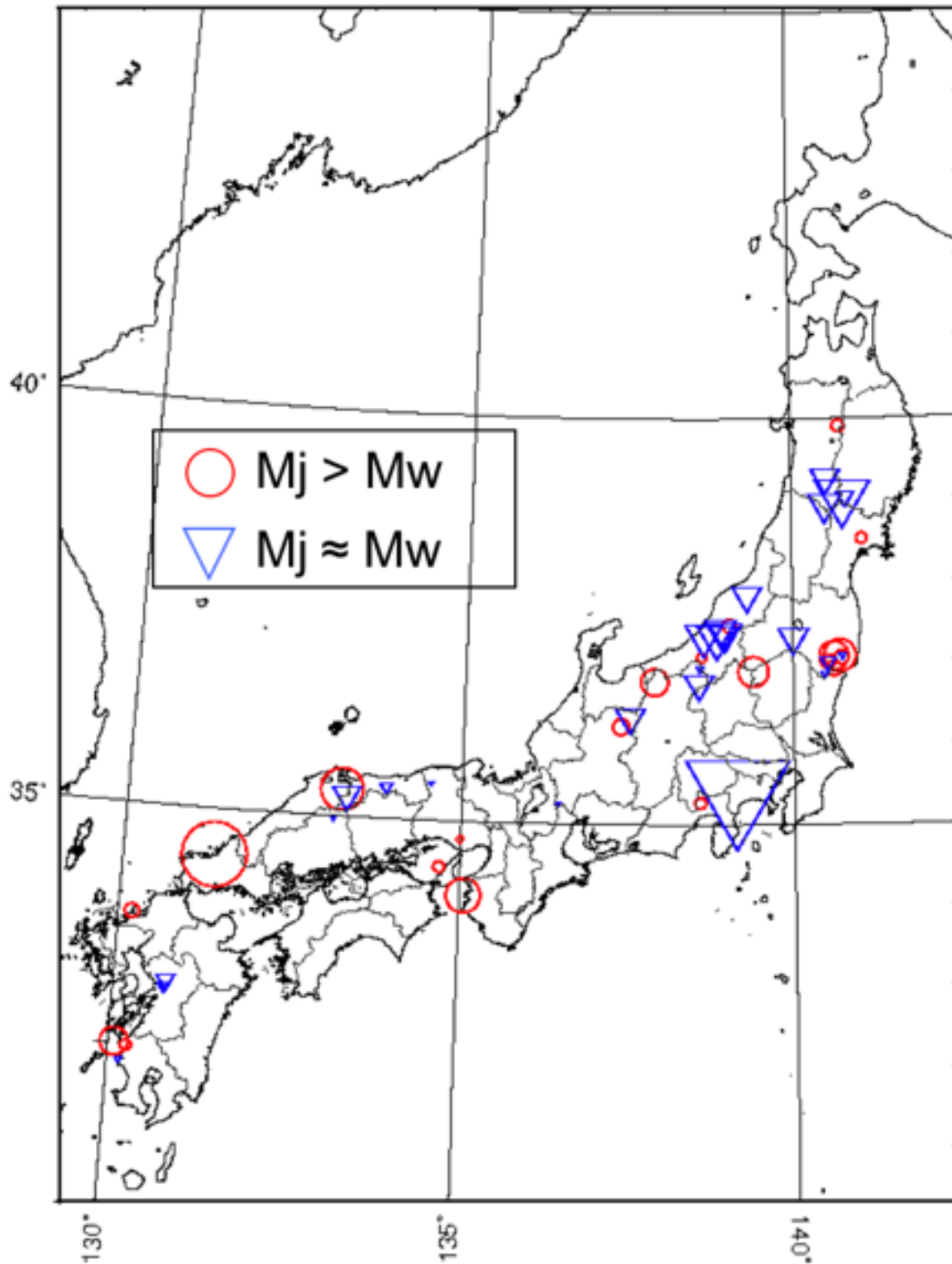
*Hiroki Kawamoto¹, Takashi Furumura¹

1. Earthquake Research Institute The University of Tokyo

In Japan, the Japan Meteorological Agency (JMA) magnitude (M_j) is officially used for the magnitude estimates of the earthquakes occurring in the area around Japan. However, it is well recognized that the estimated M_j sometimes shows large discrepancies between the moment magnitude (M_w) and momentum magnitude (M_w). Typical examples are the Western Tottori earthquake in 2000 ($M_j=7.3$; $M_w=6.8$) and Northern Yamaguchi earthquake in 1997 ($M_j=6.6$; $M_w=5.9$), all are strike-slip fault events occurred in the inland of western Japan. Since the M_j of shallow ($h < 60$ km) earthquakes are estimated by using the maximum amplitude of horizontal displacement motions recorded by long-period seismometers with a natural period of $T=5$ s, it is expecting that the propagation and attenuation properties of the long-period ground motions in this period range might be different in western Japan. In this study we examined the cause of such discrepancy between M_j and M_w occurring in western Japan based on the analysis of the K-NET and KiK-net strong ground motion data for recent shallow earthquakes.

We analyzed 47 inland earthquakes of shallow ($h < 40$ km) and large ($M_j > 5.5$) event occurred during between Sep. 1994 to Nov. 2016 in which the K-NET and KiK-net data is available. We made a regression analysis of relation between M_j and M_w , which are obtained from the JMA and the GCMT catalog, respectively. The result shows that the M_j is proportional to the M_w with a bias of 0.16 ($M_j=M_w+0.16$). After substituting this bias (0.16) from the M_j we selected the events having large discrepancy between M_j and M_w . We confirmed such peculiar events are mostly located in some area such as in Chugoku-Kinki and from South-Fukushima to South-Niigata (Fig).

To study the cause of larger M_j than M_w in western Japan we examined the strong motion record of the K-NET and KiK-net for the 2000 Western Tottori ($M_j=7.3$; $M_w=6.8$) and the 2004 Mid Niigata ($M_j=6.8$; $M_w=6.8$) earthquakes. The accelerograms of the K-NET and KiK-net are integral twice to obtain the ground displacement after applying a band pass filter ($f=0.20$ to 40 Hz) to match to the response of the JMA seismograph. Obtained waveform shows that the attenuation of the long-period ground displacement motion from the Mid Niigata earthquake is very strong with propagation in northern Japan, but it is rather weak for the Western Tottori earthquake in western Japan. It is also confirmed that the large ground displacement of the Western Tottori earthquake has strong directional dependency with larger tangential motion in the direction of fault strike and its perpendicular directions where the radiation of the SH wave from the strike-slip fault source develops large Love waves. The seismogram demonstrated that the Love wave traveling longer distances in western Japan without showing strong dispersion properties, while the development of the surface wave from the Mid Niigata earthquake is very weak in all directions. The results of this study demonstrated that the earthquakes of larger M_j , which occurred in western Japan, might be due to larger radiation of the Love wave from the source as well as efficient propagation of the short-period ($T=5$ s) Love wave in regional distances without causing significant dispersion. Such efficient Love wave propagation in western Japan might indicate the peculiarity of the crustal structure beneath western Japan compared with that of northern Japan. Such propagation and dispersion properties of the fundamental-mode, short-period ($T=5$ s) Love wave might occur due to the difference in the shallow structure such as sedimentary layers between western and northern Japan.



Numerical simulation of long-period ground motion generated from intraplate earthquakes around Ibaraki and Fukushima prefectures ~

Part III

*Fujihara Satoru¹, Fumio Kirita², Kaoru Kawaji¹, Toshihiko Yamazaki², Mitsuru Uryu², Daisuke Takekawa²

1. CTC ITOCHU Techno-Solutions, Nuclear & Engineering Department, 2. Japan Atomic Energy Agency, Construction Department

[Introduction] After the occurrence of 2011 Tohoku-Oki earthquake, phenomena of long period ground motion have been observed at seismic observation stations around the coastal region of Ibaraki prefecture for the occurrence of shallow depth intra-plate earthquakes (including 2011 Fukushima-ken Hamadori Earthquake) around Ibaraki and Fukushima prefectures. Before the occurrence of Tohoku earthquake, there was little noticeable intraplate large earthquake, and physical characteristics of generation of long-period ground motion mostly remained unclear. Therefore, better understanding nature of generation of long-period ground motion and improving seismic wave propagation around this region are very important for evaluating ground motion around the coastal region of Ibaraki prefecture. They will also lead to more reasonable evaluation of earthquake-proof safety of important infrastructures and subsurface structure around this region.

[Previous studies] In our previous studies, for achieving more accurate evaluation of seismic wave ground motion of intra-earthquakes around the coastal region of Ibaraki prefecture (strong motion, long-period ground motion, and etc), the 3-D underground structure model, which fairly explains phenomena of long-period ground motion, has been reconstructed by using postseismic events of 2011 Hamadori Earthquake. For optimizing the 3D underground structure model, we used seismic observation stations of KIK-net and Japan Atomic Energy Agency around this region. The result showed that optimized 3D structure model could better explain the generation of long-period ground motion around this region, and suggested that they are generally originated from the regional-scale characteristics of basement structure beneath intra region. Furthermore, based the finite element method using on the structure model, we performed seismic wave propagation simulation of intraplate earthquakes (moderate scale of point source, $M < 6.0$), and try to forward-model the long-period ground motion being generated during propagation thorough the inhomogeneous underground structure. Preliminary results were presented in the 2015 JPGU and 2016 JPGU.

[What we will show in this presentation] This presentation introduces the updated results our research as follows; (1) Validation tests of the 3-D underground structure model for large-scale earthquakes with finite fault model setting. We analyze several models of 2011 Hamadori Earthquake. (2) We also analyze several specific propagation properties. These include amplitude fluctuations possibly affected by source-station azimuth, source depth, specific frequency band, and so on.

Keywords: 3D structure, Seismic wave propagation, Hamadori Earthquake